The 2D Eulerian Approach of Entrained Flow and Temperature in a Biomass Stratified Downdraft Gasifier

A. Rogel and J. Aguillón

Engineering Institute of the National Autonomous University of Mexico (UNAM)
04510, Coyoacán, Mexico City, Federal District, Mexico

Abstract: This paper describes a "1-D+2-D" numerical model used to simulate the gasification of pine wood pellets in a stratified downdraft gasifier whereby Eulerian conservation equations are solved for particle and gas phase components, velocities and specific enthalpies. The model takes into account the biomass particle process such as heating up, drying, primary pyrolysis of biomass, secondary pyrolysis of tar, homogeneous reactions and heterogeneous combustion/ gasification reactions and particle size change. This CFD model can be used to predict temperature profiles, gas composition, producer gas lower heating value and carbon conversion efficiency and the reactor performance when operating parameters and feed properties are changed. The standard κ-ε and RNG κ-ε models were used to simulate the turbulent flow conditions.

Key words: CFD fixed-bed simulation, mathematical modeling, stratified downdraft gasifier, Eulerian approach, RNG κ-ε model

INTRODUCTION

Biomass and waste are widely recognized to have a major potential to be contributors to energy needs worldwide[1]. Moreover, moderate sulphur and greenhouse gas emissions associated with the use of biomass for energy production respond to the growing pressure of government policies regarding the achievement of better environmental sustainability of power generation processes in terms of air pollution control[2]. Co-combustion of biomass in pulverized coal combustors at an industrial level is a practical alternative because of the availability of biomass. Gasification enables the conversion of biomass into combustible gas, mechanical and electrical power and synthetic fuels and chemicals. Gasification is an attractive thermo chemical technology with higher efficiencies than combustion[3]. Furthermore, hydrogen produced from stratified downdraft biomass gasifiers can be utilized in fuel cells.

Gasifier simulation: To improve the thermal efficiency and predict the composition of syngas, several numeric models have been developed for biomass conversion systems. Bryden and Ragland[4] used a one-dimensional, steady-state model for a top feed, updraft, fixed bed combustor. They described the combustion of wood logs, considering drying, pyrolysis and other reactions. Cooper and Hallet[5] showed the importance of heterogeneous models in their investigation of packed-bed combustion of char, since substantial temperature differences arise between the gas and solid phase in the oxidation zone.

Very few mathematical models have coupled chemical reaction kinetics and transport phenomena to the Imbert type[6] and open core, downdraft gasifier and describe steady-state conditions[7]. Di Blasi[8] presented a heterogeneous dynamic one-dimensional model, describing heat-up-drying, primary pyrolysis of wood, secondary pyrolysis of tar and homogeneous and heterogeneous reactions. All the aforementioned investigations assumed isothermal particles.

The work of Wurzenberger *et al.* is focused on the gasification/combustion of biomass in crosscurrent moving beds, considering gradients both in the bed and inside the single particle[9]. They presented a "transient 1-D + 1-D" approach, with the gas phase within the packed bed described by 1-D Cartesian coordinates and individual particles by 1-D spherical coordinates. Their model takes into account heating up, drying, pyrolysis, secondary tar cracking, homogeneous gas reactions and heterogeneous combustion/gasification reactions.

So far, plug flow (one-directional flow) has been considered, while momentum conservation and turbulence in the fixed bed have not been taken into consideration.

The present work focuses on the construction of a dynamic "1-D + 2-D" model, taking into account the chemical and transport phenomena and turbulent kinetic energy and its dissipation in the gas flow across the biomass moving-bed, in a stratified downdraft gasifier.

Modeling: The stratified gasifier mathematical model is based on mass and energy balances within particles and is written for a one dimensional unsteady system in spherical coordinates with mass, energy and momentum

Corresponding Author: A. Rogel, Engineering Institute of the National Autonomous University of Mexico (UNAM), 04510, Coyoacán, Mexico City, Federal District, Mexico

balances for the gas phase written for a two-dimensional unsteady system in cylindrical polar coordinates. The pressure drop in the reactor is modeled using an Ergun modified equation but, given the large bed permeability, simulation can be carried out with the assumption of isobaric condition.

All relevant transport equations are solved numerically, including one for the change in particle size as particles are consumed and finite rate kinetics are included for all reactions. Published correlations are used for the transport coefficients and chemical kinetics.

Gasification: Fuel particles form a packed bed on a grate, through which ash and product gases exit. Solid particles and gas concurrent flows move slowly downwards through the gasifier. A continuous feed of fresh fuel is deposited on the bed surface and adjusted to keep the bed level constant as gasification proceeds. As the concurrent flows of biomass particles and air move downwards along the gasifier, a very complex chain of events is started, many of which can occur simultaneously, namely, heating up, drying, biomass first pyrolysis, secondary tar pyrolysis, char combustion and gasification and combustion of fuel gases, as schematically shown in Fig. 1.
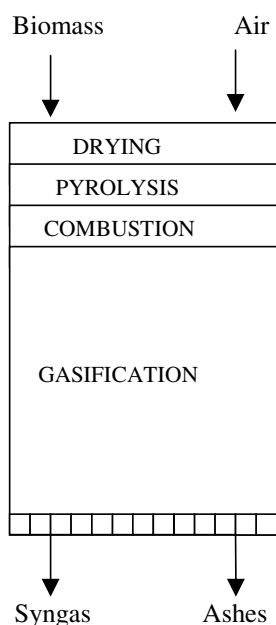

Fig. 1: Schematic of biomass gasification process in a stratified downdraft gasifier showing the principal steps (stratus): drying, pyrolysis, combustion and gasification.

Variable phase equations: In this model, which can be used for any biomass particle or gas phase property (Φ_i), the Eulerian conservation equation is

$$\frac{\partial(\rho_i r_i \Phi_i)}{\partial t} + \nabla(\rho_i r_i V_i \Phi_i) - \nabla(\Gamma_{ri} \Phi_i \nabla r_i) - \nabla(\Gamma_{\Phi i} r_i \nabla \Phi_i) =$$
$$S_{\Phi i} + D m_{j \to i} D \Phi_+ - D m_{i \to j} D \Phi_- + f_{j \to i}(\Phi_j - \Phi_i) \quad (1)$$

For the biomass solid phase, equations like (1) are solved for: two velocity components (radial and axial, in cylindrical polar coordinates), phase specific enthalpy, mass fractions of all the chemical species (row biomass, char, water and ash.). The local mean particle size is calculated from an equation of transport, as described below.

Equations like (1) are solved for: two velocity components, specific enthalpy, mass fractions of all the chemical species of the gas phase, turbulent kinetics and its dissipation rate, in accordance with the RNG κ-ε model.

In Eq. (1), Φ_+ represents the value of Φ in the mass fraction ($m_{j \to i}$) coming from phase j into phase i; similarly Φ_-. The double bar (DD) in Eq.(1) is an operator, which takes the maximum value between zero and the enclosed quantity and $f_{j \to i}$ is a friction factor coefficient for the diffusive transport of Φ between phases. For momentum equations, $f_{j \to i}$ represents the modification to the Navier-Stokes equation for flow through fixed-bed, or volume forces or the drag force on the particle; and for the enthalpy equations, the heat transfer between phases. Finally, $S\phi_i$ represents other (non-interphase) sources, for example the pressure gradients in the momentum equations.

Two diffusion terms appear in Eq. (1); the first term $\nabla(\Gamma_{ri}\Phi_i\nabla r_i)$ is the transport of Φ_i due to the turbulent diffusion or r_i in Eq. (1). The second term $\nabla(\Gamma_{\Phi i}\nabla r\Phi_i)$ is the inherent phase turbulent diffusion of Φ_i and is present only in the gas phase. This term is modeled in the same way as the single-phase cases, i.e. from the modeling of the ($V`\Phi`$) correlation (between fluctuating velocity and the fluctuating properties).

Turbulence: Longtemberg *et al.*[10] observed that at Re = 800-3344 strong eddies are very clear, caused by the strong radial flow from the middle towards the wall which "splits" up in an upward and a downward axial flow at the wall. Niven[11] stressed that in packed beds, from a plot of Ergun like equations and plotting data of several authors, the deviation from strictly laminar flow becomes significant at much lower levels, around Re = 100.

The work of Collier *et al.*[12] covers a broad set of turbulent conditions, studying heat transfer coefficient between particles in packed beds, with Re = 250-690. In the flow of air around spheres stated, Re = 100 to consider turbulent flow.

Thus an approach to studying large particles and fast heating rates as they occur in biomass gasifiers requires a detailed single particle model combined with a packed-bed reactor model which encloses mass, momentum and heat conservation equations, kinetic energy and its dissipation equations.

Fuel components: Biomass particles are considered to be composed of: row biomass, char and ash. The mass fractions of particle components (y_p^{char}, $y_p^{row\ biomass}$) are calculated by solution of equations such as those shown in (1). The ash mass fraction is determined by difference to unity.

Pyrolysis: When wood is heated, the solid discomposes by thermal scission of chemical bonds. Since the amount of volatiles can be as much as 80%[13] of the entire solid biomass, this non-oxidative process, called devolatilization or pyrolysis, has a strong influence on the whole gasification process. Species formed by this initial step may not be volatile and may undergo additional bond-breaking reactions to form volatiles or may experience condensation/polymerization reactions to form higher molecular weight products, including char. The volatiles species may undergo further reactions within the particle, either homogeneously in the gas phase or heterogeneously by reaction with the solid biomass or char. These intraparticle secondary reactions can be influenced by the rates of volatile mass transfer within and away from the particle. After escaping the particle, the tars and other volatiles may still undergo secondary reactions homogeneously in the vapor phase or heterogeneously on the surface of other biomass or char particles. Depending on reaction conditions, intra and/or extra-particle secondary reactions may exert a modest to virtually controlling influence on product yields and distribution for wood pyrolysis.

In the biomass devolatilization process, we consider that row biomass is consumed to form char in the solid phase and volatile matter in the gas phase. This process is modeled by the reaction

$$1\ kg\ raw\ biomass \rightarrow Y\ kg\ of\ volatiles + (1\text{-}Y)\ kg\ char. \quad (2)$$
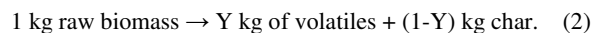
Volatile matter is considered to be a general hydrocarbon (CH_4) and the reaction rate is modeled as
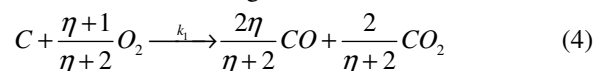
$$r_{pyrolysis} = -A_v \rho_2 y_2^{rowbiomass} \exp(-E_v / RT_2) \quad (3)$$

where A_v is a constant, ρ_2 biomass density, $y_2^{rowbiomass}$ row biomass remnant in solid phase, E_v the energy activation, R the universal gas constant (8.314 J.mol.K^{-1})and T_2 the solid phase temperature (K).

The heat of wood pyrolysis is relatively small and was investigated by Rath *et al.*[14], who report a variability of heat of reaction depending on the wood, the particle size and the final char yield. For beech, this heat of pyrolysis ranges from 150 kJ kg^{-1} d.b. at a final

char yield of about 0.18 kg kg^{-1} d.b. to -150 kJ kg^{-1} d.b. at a final char yield of 0.25 kg kg^{-1} d.b. An explanation of the changing heat of reaction may be the simultaneous occurrence of exothermic primary char production and endothermic formation of volatiles. In this work a heat neutral primary pyrolysis model is used.

Heterogeneous solid-gas reactions: Heterogeneous reactions of combustion and gasification are those of char with species in the gas phase (such as O_2, CO_2, H_2O). This work uses a simplified reaction model that considers the following overall reactions

$$C + \frac{\eta+1}{\eta+2}O_2 \xrightarrow{\ k_1\ } \frac{2\eta}{\eta+2}CO + \frac{2}{\eta+2}CO_2 \quad (4)$$

$$C + CO_2 \xrightarrow{\ k_2\ } 2CO \quad (5)$$

$$C + H_2O \xrightarrow{\ k_3\ } CO + H_2 \quad (6)$$

The ratio η of CO to CO_2 production changes with temperature, as shown in Table 1. In this Table (1-Xc)$^{1.2}$ is the amount of unreacted carbon and the empirical exponent 1.2 takes into account the change of the available reactive surface during the reactions[15].

The apparent order of reactions (4)-(6) is 1[4,7,8] and is calculated as follows:

$$r_{het} = \frac{3}{D} k_{Ti} p_i \quad (7)$$

with

$$k_{Ti} = \frac{1}{(1/k_{ci}) + (1/k_{Di})} \quad i = O_2, CO_2, H_2O \quad (8)$$

where D is the particle diameter, p_i is the partial pressure of O_2, CO_2 and H_2O and k_c and k_D are the kinetic and diffusion rates, respectively. Values for k_c and k_D are calculated by the following expressions:

$$k_c = A_h e^{-Eh/RT_2} \quad (9)$$

$$k_D = \frac{ShD_k Mc}{RT_1 D} \quad (10)$$

where *Sh* is the Sherwood number, D_k is the diffusion coefficient for O_2, CO_2 and H_2O and *Mc*, is the molecular weight of carbon. The coefficients in reactions (4)-(6) are taken from De Souza[16] (Table 1).

Particle size: Particle size changes through combustion/gasification processes. The particle size is carried out with the use of a method developed by Fueyo *et al.*[20] which is an extension of the shadow method used by Spalding. An additional scalar of solid phase Φ_s is used in the present method, which represents the inverse one of solid fraction disappeared due to mass transfer. Unlike the original method, the present method allows the selection of mass transfer processes which contributes to the particle size change.

Table 1: Kinetics expressions for heterogeneous combustion/gasification reactions

Reaction Rate	Unit	Source
$\dot{r}_1 = 1.5 \times 10^6 \exp\left(\dfrac{-13,078}{T_2}\right) p_{O_2}(1-X_c)^{1/2}$	s^{-1}	Di Blasi *et al.*[15]
$\eta = 3 \times 10^8 \exp\left(\dfrac{-30,178}{T_2}\right)$	----	Monson *et al.*[17]
$\dot{r}_2 = 4,364 \exp\left(\dfrac{-29,844}{T_2}\right) c_{CO_2}$	s^{-1}	Biggs *et al.*[18]
$\dot{r}_3 = \dfrac{k_4 p_{H_2O}}{1 + k_5 p_{H_2O} + k_6 p_{H_2}}$	s^{-1}	Mühlen *et al.*[19]
$k_4 = 4.93 \times 10^3 \exp\left(\dfrac{-18,522}{T_2}\right)$	s^{-1}bar^{-1}	Mühlen *et al.*[19]
$k_5 = 1.11 \times 10^1 \exp\left(\dfrac{-3,548}{T_2}\right)$	bar^{-1}	Mühlen *et al.*[19]
$k_6 = 1.53 \times 10^{-9} \exp\left(\dfrac{25,161}{T_2}\right)$	bar^{-1}	Mühlen *et al.*[19]

Table 2: Rate expressions for homogeneous gas-phase reactions

Reaction Rate	Unit	Source
$\dot{r}_4 = 2.78 \times 10^{-3} \exp\left(\dfrac{-1,510}{T_g}\right)\left(y_{CO} y_{H_2O} - \dfrac{y_{CO_2} y_{H_2}}{K}\right) c_{mol}^2$	Mol.m^{-3}.s^{-1}	de Souza-Santos[16]
$K = 0.0265 \exp\left(\dfrac{-65.8}{RT_g}\right)$	----	Yoon *et al.*[16]
$\dot{r}_5 = 3.98 \times 10^{14} \exp\left(\dfrac{-20,119}{T_g}\right) y_{CO} y_{O_2}^{0.25} y_{HO_2}^{0.5} c_{mol}^{1.75}$	Mol.m^{-3}.s^{-1}	Groppi *et al.*[21]
$\dot{r}_6 = 2.19 \times 10^{12} \exp\left(\dfrac{-13,127}{T_g}\right) y_{H_2} y_{O_2} c_{mol}^2$	Mol.m^{-3}.s^{-1}	Groppi *et al.*[21]
$\dot{r}_7 = 1.58 \times 10^{13} \exp\left(\dfrac{-24,343}{T_g}\right) y_{CH_4}^{0.7} y_{O_2}^{0.8} c_{mol}^{1.5}$	Mol. m^{-3}.s^{-1}	Groppi *et al.*[21]
$\dot{r}_8 = 3.21 \times 10^2 \exp\left(\dfrac{-468}{T_g}\right) y_{H2O}^{1..3} y_{CH4} c_{mol}^2$	Mol.m^{-3}.s^{-1}	Zubrin *et al.*[22]
$\dot{r}_9 = 3.21 \times 10^2 \exp\left(\dfrac{-468}{T_g}\right) y_{H2}^{1..3} y_{CO} c_{mol}^2$	Mol.m^{-3}.s^{-1}	Zubrin *et al.*[22]

The variable Φ_s is calculated from a transport equation:

$$\frac{\partial(\rho_2 r_2 \Phi_s)}{\partial t} + \nabla(\rho_2 r_2 \Phi_s V_2) - \nabla(\Gamma_{r_2} \nabla r_2) = S_{\Phi_s} \qquad (11)$$

Equation (11) includes every source associated to particle phase in all processes which do not contribute to a size change. In this work, only heterogeneous reactions are considered for mass transfer processes, in the contribution to the particle size diminution.

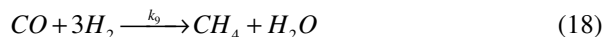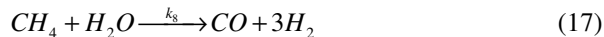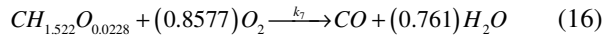After the variable Φ_s is calculated, the current mean diameter is determined by:

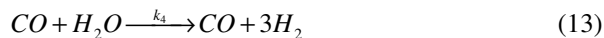$$D = D_i \Phi_s^{-\frac{1}{3}} \qquad (12)$$

where D_i is the initial particle diameter and D is the current solid diameter.

Gas components: The gas phase is modeled as a mixture of seven chemical species, represented by their mass fractions: oxygen ($y_1^{O_2}$); steam water ($y_1^{H_2O}$); carbon monoxide (y_1^{CO}); hydrogen ($y_1^{H_2}$) carbon dioxide ($y_1^{CO_2}$); a generic hydrocarbon ($y_1^{CH_4}$); and nitrogen ($y_1^{N_2}$). The transport equations as in (1) are solved for all species but the nitrogen is computed as difference from unity.

Homogeneous gas-phase reactions: Reactive gas species are produced during the drying and pyrolysis of biomass and react with each other (such as a water gas shift reaction) or with primary-air oxygen. The heat generated by exothermic reactions is important for the release of pyrolysis gases, formation of soot, or ignition

of char. In the present work the following six homogeneous reactions are considered.

$$CO + H_2O \xrightarrow{k_4} CO + 3H_2 \tag{13}$$

$$CO + 1/2O_2 \xrightarrow{k_5} CO_2 \tag{14}$$

$$H_2 + 1/2O_2 \xrightarrow{k_6} H_2O \tag{15}$$

$$CH_{1.522}O_{0.0228} + (0.8577)O_2 \xrightarrow{k_7} CO + (0.761)H_2O \tag{16}$$

$$CH_4 + H_2O \xrightarrow{k_8} CO + 3H_2 \tag{17}$$

$$CO + 3H_2 \xrightarrow{k_9} CH_4 + H_2O \tag{18}$$

Reaction (13) is an equilibrium limited reaction. At lower temperatures, it favors the production of CO_2 and H_2 and at higher temperatures CO and H_2O. The equilibrium constant K is computed from the free Gibbs enthalpies of the reaction. The equilibrium of reactions (14-18) is far on the product side and therefore, reverse reactions can be neglected. All kinetic parameters are taken from literature as given in the Table 2.

Chemical reactions rates of (13)-(18) are computed by:

$$k = \min\left(k_{Ar}, k_{EBU}\right) \tag{19}$$

where k_{Ar} and k_{EBU} are the kinetic (Arrhenius type) and turbulent mixing rates and k_{EBU} is calculated with the Eddy Break-up model (EBU):

$$k_{EBU} = C_{EBU} \frac{\varepsilon}{\kappa} \min\left(\frac{y_1^i}{S_i}, \frac{y_1^j}{S_j}\right) \tag{20}$$

where y_1^i and y_1^j are the two mass fractions of participating species in the step reaction, S_i and S_j are the associated stoichiometric coefficients and κ and ε are the turbulent kinetic energy and its dissipation rate, respectively.

Heat transfer between the particle and the gas phase: The heat flow rate in the solid-gas interphase[16] is modeled as:

$$q_{j \to i} = \frac{12.36}{D} \rho_1 Cp_1 w_1 \, Re^{-0.575} \, Pr^{-\frac{1}{3}} \left(T_j - T_i\right) \tag{21}$$

where Re and Pr are the Reynolds and Prandtl numbers for the gas phase, respectively.
ρ_1 is the gas density, Cp_1 the specific heat capacity of the gas and w_1 is the gas phase velocity.

Drag and lift forces between the particle and the gas phase: The drag and lift forces on the solid-gas interphase are modeled as follows:

$$f_{i \to j} = f_{j \to i} = \frac{3}{4D} \rho_1 C_D |V_r| \tag{22}$$

where $|V_r|$ is the relative velocity between the particle and the gas and C_D is the drag or lift coefficient, determined as:

$$C_D = \frac{24(1 + 0.15 \, Re^{0.687})}{Re} \tag{23}$$

Physical properties: Several physical data such as fuel density, thermodynamic and transport properties are required for the simulation of a biomass fuel bed. All properties are calculated depending on temperature, pressure and degree of conversion according to literature.

The density of the gas phase is given by the ideal-gas law (Eq. 24) and the density of the moisture is calculated as a function of its temperature. The enthalpy and heat capacity of the gas phase depend on temperature and gas composition, Cp =1005+(Temp1-300) Temp1 $Jkg^{-1}K^{-1}$. Viscosity is 1.8E-5 $kgms^{-1}$. Enthalpy h_k considers both, thermal and chemical enthalpy (Eq. 25):

$$\rho = \frac{p}{RT \sum_{k=1}^{n} \frac{y_k}{w_k}} \tag{24}$$

$$h_k = \Delta h_{form,k} + \int_{T^0}^{T} Cp_k \, dT \tag{25}$$

where T^0 is the reference temperature (298 K), Cp_k is the heat capacity at constant pressure for the kth species and $\Delta h_{form,k}$ is the enthalpy of formation for the kth species, defined as the heat released when a kmol of substance is reached from its former elements in the standard state. For biomass, both density (650 kgm^{-3}) and heat capacity (1112 $Jkg^{-1} K^{-1}$) are assumed to be constants and the temperature is determined from its enthalpy. The Low Heating Value (LHV) of wood is 13-15 $MJkg^{-1}$[16]. The permeability of bed (0.5) is taken as constant.

Computational methodology: The stratified downdraft gasifier is symmetrical and only half of it is simulated as two dimensional and axisymmetric in cylindrical polar coordinates. A finite volume method was employed to solve the previous transport equations, using a commercial CFD code, The PHOENICS, with an IPSA algorithm[23], was used to solve the pressure-velocity-volume fraction coupling. We used a 5x20 (radial-axial-times) mesh. In grid refinement, the result proved to be grid-independent on this mesh.

RESULTS AND DISCUSSION

Temperature profiles: The drying, pyrolysis (devolatilization) and combustion is concentrated in a narrow region at the top of the bed (0.05 0.075 m.)[6-8]. Therefore, the reduction zone determines the performance of the entire reactor. Figures 2 shows gas temperature profiles obtained from the model, compared with experimental data[15]. These are obtained by operating at an air to biomass ratio in the range of

Table 3:   Comparison between Measured and predicted composition of stratified downdraft gasifier gas

%volume	Groeneveld et al.[6]	Maunurung et al.[7]	Di Blasi et al.[8]	This work.
CO	17	18-19	18.5-20.3	20-28
H_2	14	11	9.8-16.8	5.56-10.0
CH_4	0.9	----	2.4-4.5	----
CO_2	13.6	11-13	10-16	9.78-10.75
H2O	----	----	----	10.5-11.0
N2	46.5	45-55	43-60	46.9-47.2
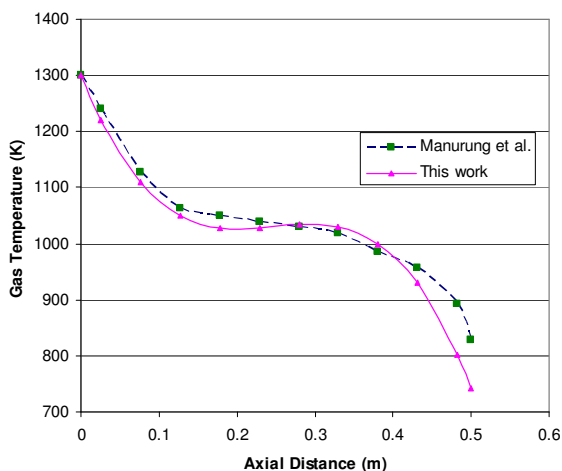
Fig. 2: Comparisons between axial gas phase temperature (Temp 1) profiles as predicted by the model (solid line) and measured by Manurung and Beenackers (dashed line)[15] for rice husk gasification. Inlet air and biomass preheat of 500 K, air to biomass ratio of 1.5 $Nm^3 kg^{-1}$ dry biomass, fuel feed rate of 15 kg hr^{-1}., bed height of 0.5 m. and fuel size 0.025 m
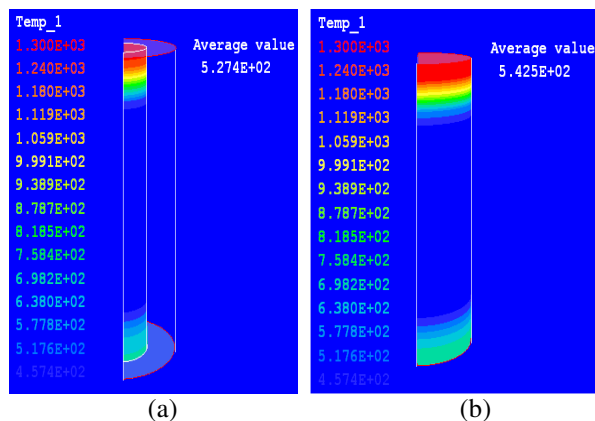
Fig. 3: Axial temperature Profile for gas phase (Temp 1) a) R=0.0625 m and b) R=0.125 m. (from PHOENICS VR VIWER, 3.5)

1.4 to 1.6 $Nm^3 kg^{-1}$ (N=Normalized) and 10-20 kg hr^{-1} of biomass. Figure 3a (R =0.0625 m.) shows how gas temperature (Temp1) rapidly reaches its maximum in the oxidation zone due to exothermic reaction of tar (CH_4) and char combustion and subsequently drops gradually down stream in the bed due to the exothermic gasification reactions and the heat loss through the reactor wall. However there is an increment in gas
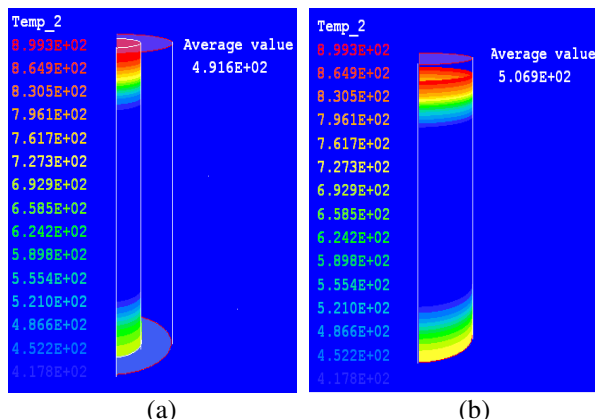

Fig. 4: Axial temperature Profile for solid phase (Temp 2) a) R=0.0625 m and b) R=0.125 m. (from PHOENICS VR VIWER, 3.5)

temperature near the gasifier bottom because the exothermic CO reduction reaction causes depletion of CO and H_2 abundant in this region of the simulation domain. This performance can be observed too in Fig. 3b, representing simulation at R=0.125m and showing variation in radial position. The model predicts this temperature behavior except at the bottom of the bed where the experimental curve is about 100 K higher. This discrepancy may be due to heat losses via the cylindrical reactor wall and the bottom grid. At oxidation zone (top of the bed) the gas temperature is around 1300 K and at temperatures bellow 1000 K, the reduction rates are so low that significant lower carbon conversion efficiencies result. Figure 4a and b show the same performance for solid phase temperature (Temp 2).

Composition profiles: As shown in Fig. 5 (R=0.125 m.) and 6(R=0.0625), the model closely predicts the composition profiles of the most relevant syngas components (CO and H_2, CO_2, H_2O) and the mass fraction of water steam is a little high. The reason behind this discrepancy is possibly due to the high water content of the biomass. Oxygen (YO2) is rapidly consumed due to combustion reaction of char and volatile matter (YCH4). Char is consumed by gasification reaction producing CO and H_2, steam reforming reaction produces CO and H_2. The high concentrations of CO and H_2 are reduced by shift reaction, CO reduction reaction and H_2 oxidation. As can be seen in Table 3, the use of reference data gives
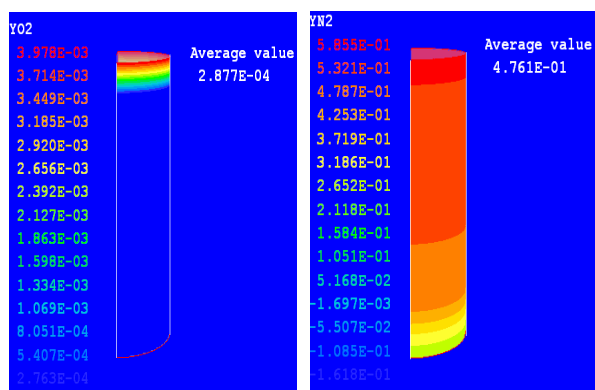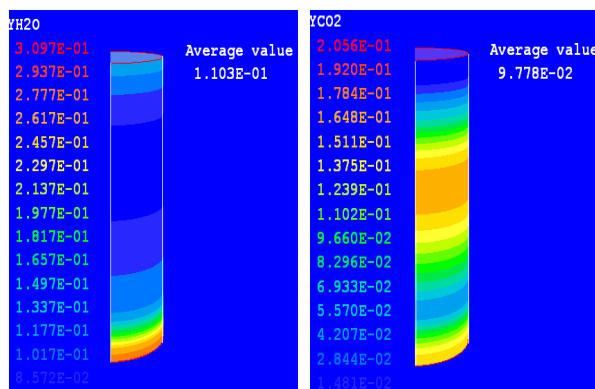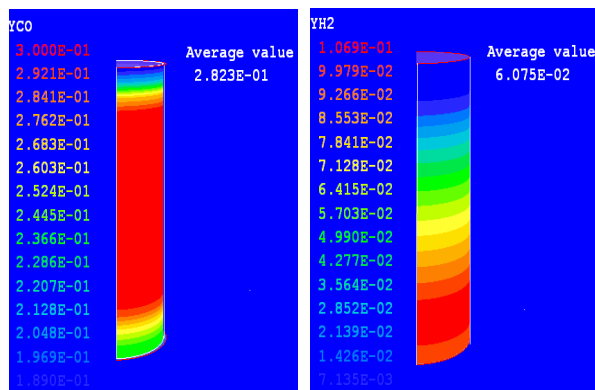
Fig. 5: Syngas composition contours in axial direction, radial position, R=0.125 m. Inlet air and biomass particles preheated at 500 K, biomass flow of 15 kg hr^{-1} $_{\text{dry biomass}}$, air to fuel ratio of 1.5 Nm^3 kg^{-1} dry biomass, bed height of 0.5 m. and fuel size 0.025 m

Fig. 6: Syngas composition contours in axial direction, radial position, R=0.0625 m. Inlet air and biomass particles preheated at 500 K, biomass flow of 15 kg hr^{-1} $_{\text{dry biomass}}$, air to fuel ratio of 1.5 Nm^3 kg^{-1} dry biomass, bed height of 0.5 m. and fuel size 0.025 m

rise to predictions of producer gas composition very close to the values reported for woody biomass by several references. It is believed that the agreement can be further improved by optimizing the model.

CONCLUSION

This paper describes the application of the Eulerian approach to a "1-D+2-D" mathematical model, which includes all the main chemical and physical processes taking place during wood pellet gasification with air in
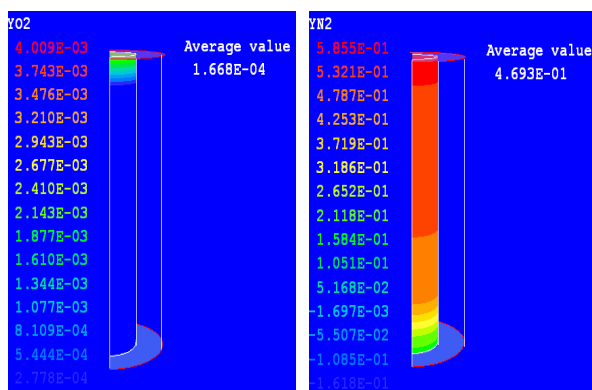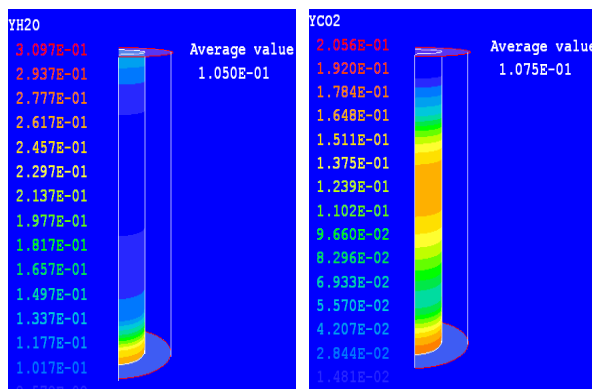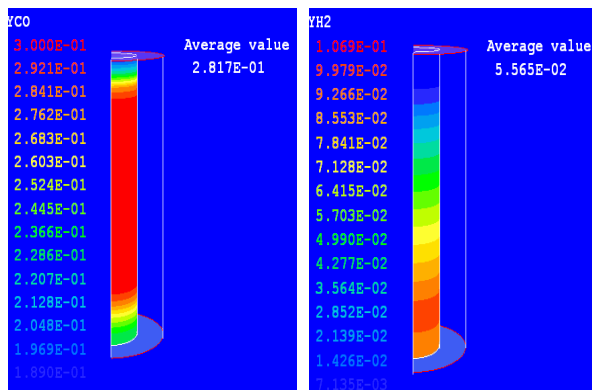
a stratified downdraft gasifier. The model is based on transient conservation equation of mass, momentum and energy, chemical kinetics, transport rates, turbulent energy and its dissipation using the RNG κ-ε model and thermodynamic relations, in cylindrical polar coordinates. The model was numerically solved using commercially available CFD code, PHOENICS. The biomass gasification process simulation using finite volume methods leads to good quantitative agreements in terms of syngas composition, gas temperature profile, biomass temperature profile and biomass

particle size change. From a qualitative point of view, the model predictions provide adequate reproduction of the dynamic behavior and the steady state configuration, on dependence on the air/biomass feed rate, of downdraft wood gasifier. Within the model there are inherent limitations and uncertainties associated with the complex process of gasification/combustion and the accuracy of measurements taken in this difficult environment; the agreement between predictions and experimental data available is qualitatively satisfactory.

ACKNOWLEDGMENTS

REFERENCES

1. Di Blasi, C., C. Branca, S. Speranoi and B. La Mantia, 2000. Drying characteristics of wood cylinders for conditions pertinent to fixed countercurrent gasification. Biomass and Bioenergy, 25: 45-58.
2. Caputo, A., M. Palumbo, M. Pelagagge and F. Scacchia, 2005. Economics of biomass energy utilization in combustion and gasification plants: Effects of logistic Variables. Biomass and Bioenergy, 28: 35-51.
3. Jong, W.U.O., J. Andries, K. Hein and H. Spliethoff, 2003. Thermo chemical conversion of brown coal and biomass in a pressurized fluidized bed gasifier with hot gas filtration using ceramic channel filters: Measurements and gasifier modeling. Appl. Energy, 74: 425-437.
4. Bryden, K.M. and K.W. Ragland, 1996. Numerical modelling of a deep, fixed bed combustor. Energy and Fuels, 10: 269-275.
5. Cooper, J. and W. Hallett, 2000. A numerical model for packed-bed combustion of char particles. Chem. Engg. Sci., 55: 4451-4460.
6. Groeveneld, M.J. and W.P.M. Van Swaaij, 1980. gasification of char particles with CO_2 and H_2O. Chem. Engg. Sci., 35: 307.
7. Manurung, R.K. and A.A.C.M. Beenackers. Modeling and Simulation of an open core downdraft moving bed rice husk gasifier. Advances in Thermochemical Biomass Conversion. London: Blackie A. & P, pp: 288-309.
8. Di Blasi, C., 2000. Dynamic behaviour of stratified downdraft gasifiers. Chem. Engg. Sci., 55: 2931-2944.
9. Wurzenberger, J., S. Wallner and H. Raupenstrauch, 2002. Thermal conversion of biomass: Comprehensive reactor and particle modeling. AICHE J., 48: 2398-2411.
10. Logtenberg, S.A. and A.G. Dixon, 1999. Computational fluid dynamics simulations of fluid flow and heat transfer at the wall-particle contact points in a fixed bed reactor. Chem. Engg. Sci., 54: 2433-2439.
11. Niven, R., 2002. Physical insight into the Ergun and Wen & Yu equations for fluid flow in packed and fluidized beds. Chem. Engg. Sci., 57: 527-534.
12. Collier, A.P., A.P. Hayhurst, S.L. Richardson and S.D. Scott, 2004. The heat transfer coefficient between a particle and a bed (packed or fluidized) of much larger particles. Chem. Engg. Sci., 59: 4613-4620.
13. Nakorn, T.W., Chutchawan, Tantakitti and S. Thavornun, 2006. Investigation of lignite and firewood co-combustion in a furnace for tobacco curing aplication. Am. J. Appl. Sci., 3: 1775-1780.
14. Rath, J., M. Wolfinger, G. Krammer, F. Barontini and V. Cozzani, 2002b. Heat of Pyrolysis. Fuel, in press.
15. Di Blasi, C., F. Buonanno and C. Branca, 1999. Reactivities of some Biomass chars in Air. Carbon, 37: 1227-1238.
16. de Souza-Santos, M., 2004. Solid Fuels Combustion and Gasification, Modeling, Simulation and Equipment Operation, Marcel Dekker, Inc., USA.
17. Monson, C.r., G.J. Germane, A.U. Blackham and l.d. Smooth, 1995. Char oxidation at elevated pressures. Combustion and Flame, 100: 669-682.
18. Biggs, M.J. and P.K. Agarwal, 1997. The CO/CO_2 product ratio for a porous char particle within an incipiently fluidized bed: A numerical study. Chem. Engg. Sci., 52: 941-952.
19. Mülhen, H.J., K.H. van Heek and H. Jüngen, 1985. Kinetic studies of steam gasification of char in the presence of H_2, CO_2 and CO. Fuel, 41: 267-278.
20. Fueyo, N., J. Ballester and C. Dopazo, 1997. The computation of particle size in Eulerian-Eulerian models of coal combustion. Intl. J. Multiphase Flow, 23: 607-612.
21. Groppi, G., E. Tronconi, P. Forzatti and M. Berg, 2000. Mathematical modeling of catalyc combustors fuelled by gasified biomass. Catalysis Today, 59: 151-162.
22. Zhubrin, S.V., 2000. Modeling of coal gasification. CHAM Ltd, PHOENICS. Demosntration case for CHAM japan.
23. Vicente, W., S. Ochoa, J. Aguillón and E. Barrios, 2003. An Eulerian model for the simulation of an entrained flow coal gasifier. Appl. Therm. Engg., 23: 1993-2008.